

**SPATIALLY-COMPRESSED CARDIAC MYOFILAMENT
MODELS GENERATE HYSTERESIS THAT IS NOT FOUND IN
REAL MUSCLE**

JOHN JEREMY RICE
YUHAI TU

*IBM T.J. Watson Research Center
Yorktown Heights, NY 10598, USA*

CORRADO POGGESI[‡]

*Dipartimento di Scienze Fisiologiche,
Viale Morgagni 63, I-50134 Firenze, Italy*

PIETER P. DE TOMBE[†]

*Department of Physiology and Biophysics,
University of Illinois Chicago, Chicago, IL 60612, USA*

In the field of cardiac modeling, calcium- (Ca-) based activation is often described by sets of ordinary differential equations that do not explicitly represent spatial interactions of regulatory proteins or crossbridge attachment. These spatially compressed models are most often mean-field representations as opposed to methods that explicitly compute the surrounding field (or equivalently, the surrounding environment) of individual regulatory units and crossbridges. Instead, a mean value is used to represent the whole population. Almost universally, the mean-field approach assumes developed force produces positive feedback to globally increase the mean binding affinity of the regulatory proteins. We show that this approach produces hysteresis in the steady-state Force-Ca responses when developed force increases Ca-affinity troponin to the degree that is observed in real muscle. Specifically, multiple stable solutions exist as a function of Ca level that could be alternatively reached depending on stimulus history. The resulting hysteresis is quite pronounced and disagrees with experimental characterizations in cardiac muscle that generally show little if any hysteresis. Moreover, we provide data showing that hysteresis does not occur in carefully controlled myofibril preparations. Hence, we suggest that the most widely used methods to produce multiscale models of cardiac force generation show bistability and hysteresis effects that are not seen in real muscle responses

[‡]Work partially supported by MUR (PRIN2006) and Università di Firenze (ex-60%).

[†]Work partially supported by NIH grants HL-62426 (project 4), HL-75494 and HL73828.

1. Introduction

As described in a previous review [1], there are still difficulties in developing predictive myofilament models given that the underlying muscle biophysics has yet to be fully resolved. Another difficulty lies in trying to compress the spatial aspects of myofilaments at the molecular level into a tractable system of equations. Partial differential equations or Monte Carlo approaches are typically required for explicit consideration of the spatial interactions, whereas spatially-compressed sets of ordinary differential equations (ODEs) are required for computational efficiency to allow large-scale multicellular models.

The spatially compressed models can be termed mean-field as opposed to methods that explicitly compute the surrounding field (environment) of individual regulatory units and/or crossbridges; instead, a mean value is used to represent the whole population. The most widely used approach is that force/activation level produces positive feedback to globally increase the mean binding affinity of the regulatory unit (troponin/tropomyosin). The mean-field approach is used in almost all ODE-based modeling efforts from diverse research groups. Recent examples are refinements of earlier models (e.g., [2-4]). We construct a generic version of this approach and show that hysteresis and bistability can result from this construction.

2. Method

Most myofilament models contain a strong positive feedback of muscle activation to increase Ca binding to regulatory units. This feedback plays a dual role in both simulating experimental observed increases in Ca affinity and providing a mechanism to produce steep Ca sensitivity and high apparent cooperativity (often in conjunction with other mechanisms). A typical mean-field approach to modeling cardiac myofilaments is shown in Fig. 1A. Here the state names are coded with 0 for no Ca bound or 1 for Ca bound in the first character. The second character is W for weakly-bound (non-force generating) or S for strongly-bound (force generating) crossbridges. Activation occurs as increasing [Ca] will cause transition from the rest state (0W) to a Ca-bound state that is still weakly bound (1W). Transitions between weakly- and strongly-bound states are controlled by constants f and g that represent apparent weak-to-strong binding transition as typically defined in two-state crossbridge schemes. Note that the right-hand side has only the crossbridge detachment step that illustrates an implicit assumption which is that crossbridges do not strongly bind and generate force when no Ca is bound to the associated regulatory proteins.

Very similar approaches have been employed and explained in depth elsewhere (e.g., [5, 6]). For the remainder of the paper, we will refer to the approach as global feedback on Ca-binding affinity (GFCA).

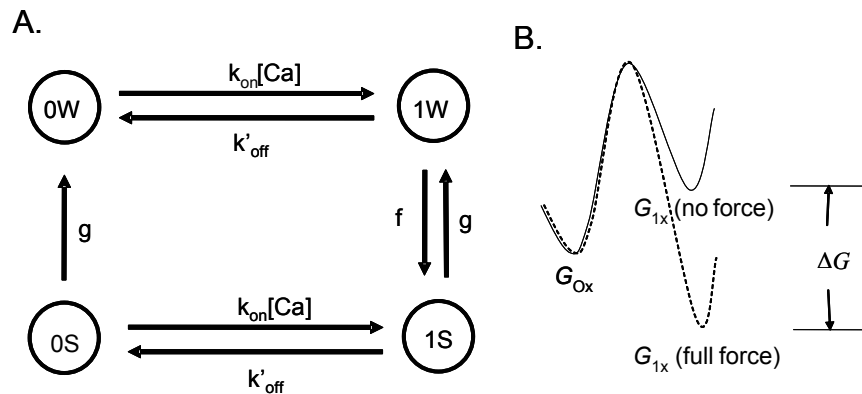


Figure 1: Generic model of force feedback on Ca binding. A. State diagram with transition rates. B. Schematic of assumed energy diagram for Ca binding where the free energy of the Ca-bound state is assumed to decrease as the model transitions from no force to full force.

For the model shown, the normalized developed force can be computed as fraction of strong bound crossbridges as shown below

$$FractSBXB = \frac{0S + 1S}{f / (f + g)} \quad (1)$$

where 0S and 1S refer to the fractional occupancy of the respective states and the denominator is the theoretical fraction of strongly-bound crossbridge for the limiting case of high [Ca] conditions (hence, only states 1W and 1S are populated).

The Ca binding is described by the left to right transitions. Ca binding is assumed to be more complicated than a simple buffer in that the dissociation constant is a function of the developed force. Specifically we assume the following formulation

$$K_d' = \frac{k_{off}'}{k_{on}} = \frac{k_{off}}{k_{on}} e^{\frac{\Delta G FractSBXB}{RT}} \quad (2)$$

where ΔG is the change in free energy of the Ca-bound state as the system transitions from no force to fully developed force (see Fig. 1B). The other constants are the Universal Gas Constant (R) and the absolute temperature (T).

The forward transition k_{on} is assumed fixed because Ca binding is generally assumed to be diffusion limited. In contrast, the backward transition k'_{off} is assumed to be a function of developed force. As *FractSBXB* transitions from a minimum value of 0 to a maximum value of 1, k'_{off} will decrease from the default value equal k_{off} to the minimum value of $k_{off} \exp(-\Delta G/RT)$. For the simulation shown the default values of the parameters are $k_{on} = 50 \mu\text{M}^{-1} \text{s}^{-1}$, $k_{off} = 500 \text{s}^{-1}$, $f = 40 \text{s}^{-1}$ and $g = 10 \text{s}^{-1}$. Similar values are used in previous studies and are justified elsewhere [5, 6].

3. Results

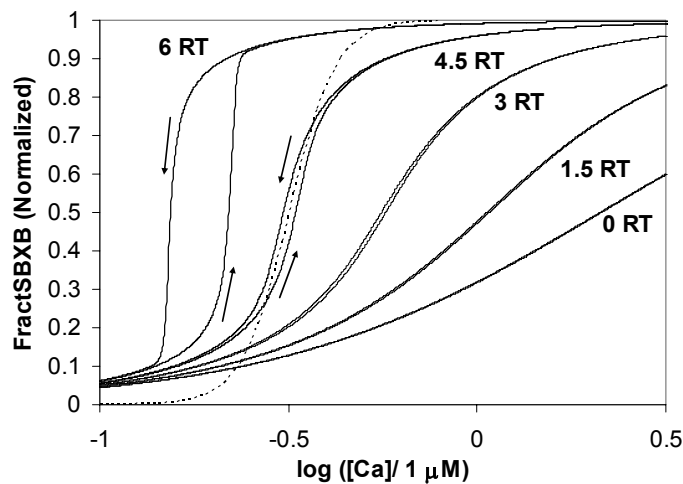


Figure 2: Pseudo-steady-state responses for the generic GFCA model for varying levels of ΔG as labeled. Increasing ΔG produces both an increase in apparent cooperativity and also leads to hysteresis. The dashed trace shows a true Hill function with $N_H = 7$ similar to what is measured experimentally for real muscle [7, 8].

3.1. Pseudo-steady-state solution

The system shown in Fig. 1 can be solved for the approximate steady-state response by slowly increasing the $[\text{Ca}]$ (-3 to 3 in units of $\log([\text{Ca}]/1 \mu\text{M})$) over 160 s so that the model is in approximate steady-state conditions. The $[\text{Ca}]$ is lowered from the maximum values over the next 160 s to check for hysteresis. As shown in Fig. 2, the steady-state Force-Ca (F-Ca) relation increase in steepness and apparent cooperativity with ΔG . When the $\Delta G = 4.5\text{RT}$, the middle part of the curve has a steepness that approximates real cardiac muscle that has a Hill coefficient (N_H) of approximately 7 for sarcomere lengths (SLs) in the range of 1.85-2.15 μm [7]. Note that the shape of the model F-Ca

relation deviates from that of a true Hill function ($N_H = 7$) as shown by the dashed line. Specifically, the model response shows relatively little apparent cooperativity in the low [Ca] and high [Ca] regimes with the most steepness near the mid-force regions. In fact, increasing the level of GFCA by setting $\Delta G = 6$ RT will increase the steepness in the mid-force regions but does little to increase the apparent cooperativity outside this regime. Such behavior has been described before as generic behavior of the GFCA models, and thus may hamper their appropriateness model for simulating real muscle responses [1]. However, the focus of the paper here is on the hysteresis that can occur when the GFCA is strong. Note that little or no hysteresis is seen for $\Delta G = 3.0$ RT, 1.5 RT or 0 RT. However these lower values do not generate steep enough F-Ca relations to replicate real muscle response as seen in the literature (e.g., [7-9]).

3.2. *True steady-state solution*

The hysteresis behavior shown in Fig. 2 could potentially be an artifact of not reaching steady state in the traditional sense of $t \rightarrow \infty$. Similar effects can often be seen in models when [Ca] is changed too quickly. We analyzed the true steady-state response using AUTO as part of the XPPAUT software package[§]. Briefly, AUTO implements continuation methods that compute a family of fixed points of a non-linear system as one or more parameters are varied. Commonly, continuation methods start at an initial fixed point and then use the system Jacobian to extend the solution as parameters are varied. Iteration produces a continuous family of fixed points, and Jacobian singularities signal bifurcations.

Figure 3B shows that true steady-state hysteresis does occur for values of ΔG in the range of 5.791 to 6.048 RT. The data correspond to one [Ca] level, but the general behavior is found for [Ca] values near the Ca_{50} with similar values of ΔG . The effects of the two stable solutions are illustrated in Fig. 3B where the model is started at either high or low force levels. The upper trace for $\Delta G = 6$ RT is producing more force for lower [Ca] compared to the lower trace which is started at the lower force level. Moreover, the lower traces $\Delta G = 6$ RT show extreme parameter sensitivity as the steady-state solution may change branches on the bifurcation diagram in Fig. 3A.

For lesser values of ΔG , while true steady-state hysteresis is not found, one can still observe that the model takes several seconds to reach steady-state. As

[§] <http://www.math.pitt.edu/~bard/xpp/xpp.html>

shown in Fig. 3B, the $\Delta G = 4.5$ RT take relatively long to settle to a steady-state value near 50% force. The long time to reach steady state is not intuitive given that all model rate constants are $\geq 10 \text{ s}^{-1}$, suggesting a time constant of relaxation on the order of 100 ms. Moreover, the delay also shows why hysteresis effects can appear in the $\Delta G = 4.5$ RT trace in Fig. 2. Note that hysteresis appears in pseudo-steady-state response in Fig. 2 but not true steady-state in Fig. 3. Hence, for biological systems that have finite lifetimes (especially for *in vitro* preparations where data collection is limited), a long-time to settle to steady state may produce hysteresis-like effects even if not in the traditional sense of $t \rightarrow \infty$.

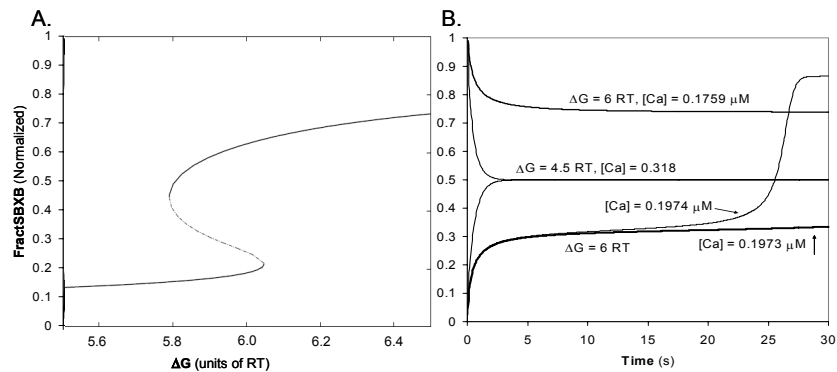


Figure 3: A. Bifurcation diagram shows true-steady responses for the generic GFCA model for ΔG as varied along the abscissa ($[Ca] = 0.195 \mu M$). Between limit points at 5.791 and 6.048 RT, two stable solutions are found with one unstable as shown by the dashed line. B. Time traces illustrate step responses starting at either 0 or full force. The $\Delta G = 4.5$ RT traces do not show hysteresis. In contrast, $\Delta G = 6.0$ RT traces show hysteresis effects and extreme parameter sensitivity. Note that essentially the same hysteresis effects are found in A using continuation methods and in B using ODE integration. Hence, the hysteresis cannot be an artifact of a particular numerical method.

3.3. Comparison to other models

Several published models show similar behavior to the generic model developed above. As an example, Fig. 4 shows a simulated F-Ca relation for the model proposed in [4] for $SL = 1.8, 2.0$ and $2.2 \mu m$. In this model, the actual change in Ca-binding affinity is roughly 20 fold. In addition, the change in Ca-affinity is assumed to increase using a Hill-like function ($N_H = 3.5$) of the concentration of strongly-bound crossbridges. Note that a 20-fold change in affinity corresponds to $\Delta G = 3$ RT which does not produce substantial hysteresis in the generic model (see Fig. 2). However, the additional nonlinearity in the Hill function generates the higher level of hysteresis seen in Fig. 4. While we

have not reprinted data here, the model in [4] shows true steady-state hysteresis when stepped to different levels of $[Ca]$ (compare $SL = 1.7 \mu M$ trace in Fig. 6 in [4] with the data in Fig. 3B; the $SL = 2.2 \mu M$ trace is operating higher on the F-Ca relation where hysteresis is not seen).

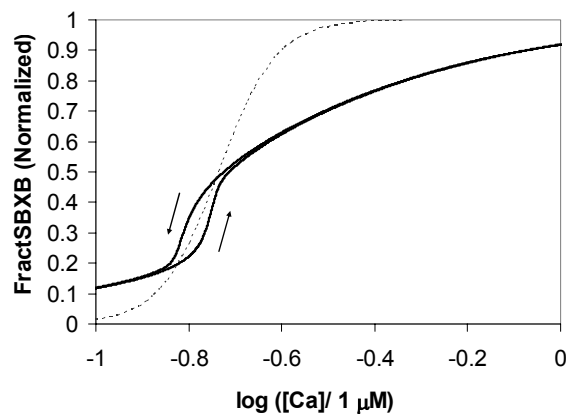


Figure 4: The F-Ca relation of the Yaniv et al. model [4] for $SL = 1.8, 2.0$ and $2.2 \mu M$ (traces essentially overlap) show clear hysteresis as seen in the generic model in Fig. 1. The protocol is the same as in Fig. 2. The dashed trace shows a true Hill function with $N_H = 7$ similar to what is measured experimentally for real muscle [7, 8].

4. Discussion

4.1. Implications of modeling results

The modeling formalism, shown in Fig. 1, is developed here as the most generic formulation of GFCA. As shown in the previous sections, the approach generalizes to published models and also represents the mean-field approximation of the spatially-explicit approaches [10]. However, GFCA produces steady-state F-Ca relations that deviate substantially from true Hill functions in ways that real muscles do not, i.e., are too steep at mid-level $[Ca]$ and not cooperative enough at low and high $[Ca]$ regimes (see Figs. 2 and 4).

If GFCA is the only cooperative mechanism in a model, then the assumed change in Ca-binding affinity is much larger than experimental estimates. Specifically, experimental estimates suggest a maximal affinity change of 15-20 fold [1, 5, 6]. In contrast, the results in Fig. 2 suggest a change of approximately 90 fold is required to replicate the degree of cooperativity seen in real F-Ca relations. This finding casts doubt on the ability to produce models

with realistic Ca sensitivity when GFCA is the only cooperative mechanism, as is the case for some published models.

While GFCA may be insufficient to generate steep enough F-Ca relations, one might assume that other cooperative mechanisms could be added to improve the steepness of F-Ca relations. This approach has been tried in many published modeling efforts (e.g., [3, 5, 11]). However, adding even a small amount of GFCA can produce the undesirable effects of increasing apparent cooperativity at mid-level [Ca] but not at low and high [Ca] regimes [1, 5]. As a specific example, compare F-Ca results for models with GFCA (M1 and M2) with the model without (M5) in Fig. 5 of Schneider et al. [11]. Only models without GFCA seem to be able to produce F-Ca relations that resemble a Hill function as seen in real muscle. While a complete analysis of all published models is not possible here, we suspect that adding GFCA with other cooperative mechanisms can also produce marked bistability in the F-Ca relation (e.g., model in Fig. 4 has additional Hill-like cooperative effects in Ca binding). As the next section discusses, high levels of bistability do not generally agree with experiment results.

The modeling results here are for steady-state [Ca] and fixed muscle lengths. In a real contracting ventricle, both [Ca] and muscle length will be varying with time so that hysteresis effects may be masked. However, the dynamic responses of muscle are strongly affected by the steady-state Ca sensitivity, and GFCA has been proposed to produce activation and relaxation kinetics that are slower in models than in real muscle [1, 5]. Figure 3B explicitly shows this slowing for a step response in Ca level. We envision pathological conditions (e.g., congestive heart failure) for which a prolonged Ca transient and/or increased diastolic transient could unmask the hysteresis.

4.2. *Experimental evidence of hysteresis*

Experimental evidence for hysteresis in the activation of the myofilament was first reported in single muscle fibers of the barnacle by Ridgway *et al.* [12]. The fibers were either micro injected with aquorin to measure intracellular calcium and electrically stimulated or chemically permeabilized (skinned) by treatment with detergent. In both cases, these investigators found larger force at equivalent levels of activator Ca when the muscle had first experienced a higher level of contractile activation. Brief periods of full relaxation, on the other hand, were sufficient to eliminate this “memory” or hysteresis effect. A follow up study by Brandt *et al.*, however, failed to confirm these results in skinned vertebrate skeletal muscle fibers [13]. Another phenomenon that may, or may

not, be related to hysteresis is stretch activation in skeletal muscle, first described by Edman *et al.* [14]. Here, a tetanized single skeletal muscle is stretched, relatively slowly, for a brief period and then returned to the original muscle length. The stretch resulted in a change in tetanic force precisely as predicted by the active force-length relation. However, sustained elevated tetanic force is found only following the brief stretch-release maneuver on the descending limb of the force-SL relationship, and hence, is unlikely to occur in cardiac tissue that does not operate on the descending limb (see [1]).

The most comprehensive, and to our knowledge only, study on myofilament activation hysteresis has been reported by Harrison *et al.* [15]. In that study, skinned rat myocardium was sequentially immersed into solutions containing varying amounts of activator Ca. Similar to the Ridgway *et al.* study, prior exposure to a high [Ca] led to an apparent left shift of the F-Ca relationship consistent with an increase in overall myofilament Ca sensitivity. Interestingly, this phenomenon was most pronounced at short SLs and virtually disappeared at $SL > 2.1 \mu\text{m}$ (i.e., lengths for which actin double overlap is no longer present). Moreover, osmotic compression of the myofilament lattice by application of dextran, a high molecular weight compound that cannot enter the space between contractile filaments [16, 17], eliminated hysteresis. Based on the SL dependence of hysteresis and its elimination by osmotic compression, these authors speculated that prior activation at the higher Ca levels induced a persistent reduction in inter-filament spacing to increase Ca sensitivity. Although not the specific focus of our studies, we have nevertheless not found evidence for hysteresis in inter-filament spacing as measured by x-ray diffraction in either intact or skinned isolated skeletal or cardiac muscle [16-19].

Studies on both intact [20-22] and skinned [7, 23] myocardium do not find evidence for hysteresis in F-Ca relationships, albeit hysteresis was not the primary focus of these studies. Likewise, intact cardiac trabeculae with pharmacologically slowed Ca transients show prolonged relaxations that occur along a single F-Ca relation that is independent of the preceding developed force (see Figs. 5-6 in [9] and Fig. 6 in [24]). Finally, hysteresis of the type referred to above as “stretch activation” is expected to lead to a significant phase shift in sinusoidal perturbation analysis experiment at frequencies close to DC. Although there is some indication in skeletal muscle for such a phenomenon [25, 26], this has not been observed in isolated cardiac muscle [27-30].

We propose that the controversial hysteresis finding above may result from inadequate control of the ionic environment surrounding the myofilaments.

Specifically, diffusion delays in activation-relaxation dynamics are a significant limitation associated with the study of large isolated fibers (such as the barnacle single fiber) or multi-cellular isolated cardiac muscle. Hence, rapid changes in $[Ca]$ in the bathing solution surrounding these muscles do not translate in equal changes in activator Ca as sensed by troponin. For this reason, the single myofibril rapid solution change technique has been widely adopted to study skeletal and cardiac muscle activation-relaxation dynamics [29, 31-36]. This technique employs single myofibrils or small bundles of myofibrils ($\sim 1\text{-}5\ \mu\text{m}$ average diameters) that are mounted between two glass micro-pipettes; the ionic environment can be altered within $\sim 5\ \text{ms}$ by rapid solution switching. The short diffusion pathway coupled with continuous superfusion produce essentially no ambiguity in the ionic environment surrounding the myofilaments.

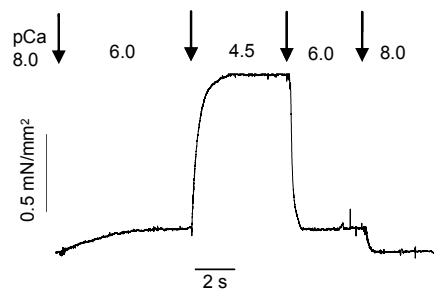


Figure 5: Activation-relaxation cycles recorded in human atrium cardiac muscle (15°C ; initial $SL = \sim 2.2\ \mu\text{m}$). Activator $[Ca]$ is altered rapidly (within $5\ \text{ms}$) by rapid solution switching techniques. The actual $[Ca]$ applied is as indicated in the figure in pCa units ($pCa = -\log([Ca]/1\ \text{M})$). Similar to previous studies in skeletal muscle [33, 34, 36, 37], there is no apparent hysteresis in myofilament steady-state force level. Unpublished results from the laboratory of C. Poggesi.

As seen in Fig. 5, hysteresis in myofilament steady-state activation level cannot be readily detected and hence is small if extant. These data can be qualitatively compared to Fig. 4B that shows pronounced history dependence for $\Delta G = 6\ RT$ (see also Fig. 6 in [4]). Also, there is no variation in the kinetic parameters of myofilament activation. Thus, the rate of force development is a direct function of the $[Ca]$, being faster at higher $[Ca]$, regardless of the activation history that precedes the switch to a particular $[Ca]$. Furthermore, the rate of force relaxation is relatively slow and not affected by the level of Ca activation from which relaxation is initiated [33, 34, 36, 37]. Overall, these experiments suggest that there is little, if any, hysteresis in myofilament Ca activation.

5. Conclusion

The paper has shown that bistability and hysteresis in the F-Ca response is an inherent behavior in models with high levels of GFCA. We have also shown that such behaviors can result with lesser amounts of GFCA when other cooperative mechanisms are represented. In contrast, experimental data suggests little or no hysteresis in real muscle responses. Hence, one should consider these effects when using spatially compressed ODE-based models that include GFCA. Moreover, the ODE-based models are often developed to combine single cells into multiscale tissue-level models. If bistability and hysteresis exist in the single cells, one could envision situations in which the stability of larger scale models could be adversely affected because individual cells can reach multiple stable steady-state forces depending on small changes in the stimulus and environment histories of each cell.

References

1. J.J. Rice & P.P. de Tombe, *Prog Biophys Mol Biol.* 85, No. 2-3, 179-95 (2004).
2. L.B. Katsnelson & V.S. Markhasin, *J Mol Cell Cardiol.* 28, No. 3, 475-86. (1996).
3. S.A. Niederer, P.J. Hunter & N.P. Smith, *Biophys J.* 90, No. 5, 1697-722 (2006).
4. Y. Yaniv, R. Sivan & A. Landesberg, *Am J Physiol Heart Circ Physiol.* 288, No. 1, H389-99. (2005).
5. J.J. Rice, R.L. Winslow & W.C. Hunter, *Am J Physiol.* 276, No. 5 Pt 2, H1734-54 (1999).
6. A. Landesberg & S. Sideman, *Am J Physiol.* 266, No. 3 Pt 2, H1260-71 (1994).
7. D.P. Dobesh, J.P. Konhilas & P.P. de Tombe, *Am J Physiol Heart Circ Physiol.* 282, No. 3, H1055-62 (2002).
8. J.C. Kentish & A. Wrzosek, *J Physiol.* 506, No. Pt 2, 431-44. (1998).
9. L.E. Dobrunz, P.H. Backx & D.T. Yue, *Biophys J.* 69, No. 1, 189-201 (1995).
10. J.S. Shiner & R.J. Solaro, *Biophys J.* 46, No. 4, 541-3. (1984).
11. N.S. Schneider, T. Shimayoshi, A. Amano & T. Matsuda, *J Mol Cell Cardiol.* 41, No. 3, 522-36 (2006).
12. E.B. Ridgway, A.M. Gordon & D.A. Martyn, *Science.* 219, No. 4588, 1075-7. (1983).
13. P.W. Brandt, B. Gluck, M. Mini & C. Cerri, *J Muscle Res Cell Motil.* 6, No. 2, 197-205. (1985).

14. K.A. Edman, G. Elzinga & M.I. Noble, *J Gen Physiol.* 80, No. 5, 769-84. (1982).
15. S.M. Harrison, C. Lamont & D.J. Miller, *J Physiol.* 401, No., 115-43. (1988).
16. J.P. Konhilas, T.C. Irving & P.P. de Tombe, *Circ Res.* 90, No. 1, 59-65. (2002).
17. G.P. Farman, J.S. Walker, P.P. de Tombe & T.C. Irving, *Am J Physiol Heart Circ Physiol.* 291, No. 4, H1847-55 (2006).
18. G.P. Farman, E.J. Allen, D. Gore, T.C. Irving & P.P. de Tombe, *Biophys J.* 92, No. 9, L73-5 (2007).
19. T.C. Irving, J. Konhilas, D. Perry, R. Fischetti & P.P. de Tombe, *Am J Physiol Heart Circ Physiol.* 279, No. 5, H2568-73. (2000).
20. H.E. ter Keurs, W.H. Rijnsburger, R. van Heuningen & M.J. Nagelsmit, *Circ Res.* 46, No. 5, 703-14. (1980).
21. P.P. de Tombe & H.E. ter Keurs, *J Physiol.* 454, No., 619-42 (1992).
22. P.P. de Tombe & H.E. ter Keurs, *Circ Res.* 66, No. 5, 1239-54. (1990).
23. J.C. Kentish, H.E. ter Keurs, L. Ricciardi, J.J. Bucx & M.I. Noble, *Circ Res.* 58, No. 6, 755-68 (1986).
24. P.H. Backx, W.D. Gao, M.D. Azan-Backx & E. Marban, *J Gen Physiol.* 105, No. 1, 1-19 (1995).
25. M. Kawai & P.W. Brandt, *J.Muscle.Res.Cell Motil.* 1, No., 279-303 (1980).
26. M. Kawai & Y. Zhao, *Biophysical Journal.* 65, No., 638-51 (1993).
27. T. Wannenburg, G.H. Heijne, J.H. Geerdink, H.W. Van Den Dool, P.M. Janssen & P.P. De Tombe, *Am J Physiol Heart Circ Physiol.* 279, No. 2, H779-90 (2000).
28. K.B. Campbell, M.V. Razumova, R.D. Kirkpatrick & B.K. Slinker, *Biophys J.* 81, No. 4, 2278-96 (2001).
29. M. Chandra, M.L. Tschirgi, S.J. Ford, B.K. Slinker & K.B. Campbell, *Am J Physiol Regul Integr Comp Physiol.* [Epub ahead of print], No. (2007).
30. M. Kawai, Y. Saeki & Y. Zhao, *Circ Res.* 73, No. 1, 35-50. (1993).
31. R. Stehle, M. Kruger & G. Pfitzer, *Biophys J.* 83, No. 4, 2152-61. (2002).
32. P.P. de Tombe, A. Belus, N. Piroddi, B. Scellini, J.S. Walker, A.F. Martin, C. Tesi & C. Poggesi, *Am J Physiol Regul Integr Comp Physiol.* 292, No. 3, R1129-36 (2007).
33. C. Tesi, F. Colomo, S. Nencini, N. Piroddi & C. Poggesi, *Biophys J.* 78, No. 6, 3081-92 (2000).
34. C. Tesi, N. Piroddi, F. Colomo & C. Poggesi, *Biophys J.* 83, No. 4, 2142-51 (2002).
35. K.B. Campbell, M.V. Razumova, R.D. Kirkpatrick & B.K. Slinker, *Ann Biomed Eng.* 29, No. 5, 384-405 (2001).
36. C. Poggesi, C. Tesi & R. Stehle, *Pflugers Arch.* 449, No. 6, 505-17 (2005).
37. C. Tesi, F. Colomo, S. Nencini, N. Piroddi & C. Poggesi, *J Physiol.* 516, No. Pt 3, 847-53. (1999).